

Rheological fluid motion in tube by metachronal wave of cilia

S. Maiti *, S. K. Pandey †

Department of Applied Mathematics

*Indian Institute of Technology (Banaras Hindu University),
Varanasi-221005, India*

Abstract

The purpose of this paper is a theoretical study of a non-linear problem of rheological fluid transport in an axisymmetric tube by cilium. However, an attempt has been made to explain the role of cilia motion on the transport of fluid through the ductus efferentes of the male reproductive tract. Ostwald-de Waele power law viscous fluid has been considered to represent the rheological fluid to analyze pumping by means of a sequence of beat of cilia from row to row of cilia in a given row of cells and from one row of cells to the next (metachronal wave movement) under conditions for which the corresponding Reynolds number is small enough for inertial effects to be negligible and the wavelength to diameter ratio is large enough for the pressure to be considered uniform over the cross-section. Analyses and computations of the detailed fluid motions reveal that the time-averaged flow rates are directly dependent on ϵ , a non-dimensional measure involving the mean radius R of the tube and the cilia length. Thus, flow rate significantly varies with the cilia length. Moreover, the flow rate has been reported close to the estimated value 6×10^{-3} ml/h in human ductus efferentes when ϵ is near by 0.5. The estimated value was suggested by Lardner and Shack [4] in human based on the experimental observations on the flow rates in the ductus efferentes in the other animals, e.g., rat, ram, and bull. In addition, the nature of the rheological fluid, i.e., the value of the fluid index n strongly influences various flow-governed characteristics.

Keywords: Non-Newtonian Fluid; Cilia Movement; Metachronal Wave; Flow Reversal; Velocity at Wave Crest and Trough.

*Email address: maiti000000somnath@gmail.com/somnathm@cts.iitkgp.ernet.in (S. Maiti)

†Email address: skpandey.apm@itbhu.ac.in (S. K. Pandey)

1 Introduction

A cilium which means an eyelash in Latin, is motile (although not all cilia motile) hairlike slender appendage/sprotuberance that project from the free surfaces of certain cells (e.g. eukaryotic cells) and is present in almost all groups of the animal kingdom. Because of its motility, it plays an important role in diverse physiological processes such as locomotion, alimentation, circulation, respiration and reproduction.

There are two types of cilia namely motile cilia and non-motile or primary cilia. However, the motile cilia which do not beat randomly but are coordinated are taken into consideration in this study. This nature of the cilia gives extremely interesting aspects of ciliated epithelium. A summary of general observations and conclusions on the cilia of the gill of several aquatic species was given by Rivera [1] as: (a) In any given tissue, the rate of beat of all the cilia is remarkably uniform. (b) The lashings of a single cilium and of cilia on adjacent cells appear to be definitely coordinated. (c) A definite metachronal wave is established. Metachronal rhythm is a movement where there is always a sequence of beat from row to row of cilia in a given row of cells and from one row of cells to the next, so that any small foreign body resting on the ciliated surface is progressively moved always in the same direction.

Since a metachronal wave provides a more “steady progression of water over the ciliated surface or perhaps because it is not practical to excite a synchronous beat over a large area” (Sleigh [9]), it is widely believed that cilia beat in a metachronal wave rather than synchronously. However, the metachronal wave along a ciliated surface can change its pattern (Sleigh [9]). The change depends on whether the metachronal waves travel in the same direction as the effective stroke of the ciliary beat (symplectic metachronism), or the metachronal waves travel in the opposite direction to the effective stroke of the beat and thus opposite to the movement of fluid (antiplectic metachronism), or the cilia beat at right angles to the line of wave progression (diaplectic metachronism). Satir [8] showed an example of a diaplectic metachronal wave in Figure 6 of his study [8], while some data based on wave lengths, metachronal wave velocities and frequencies are available for lower animal forms (Sleigh [9]). It is to be noted that data do not appear to be readily obtainable for higher animal species, especially mammals. However, it was measured that the beat frequency for cilia lining in the rabbit oviduct is approximately 20-30 beats/sec (Borell et al. [11]). It is important to mention that this order of magnitude of the frequency is comparable with frequencies of cilia beat of lower forms (Sleigh [9]).

It is to be noted that the investigations on the hydrodynamics of protozoa which use cilia

for locomotion have being carried out by many investigators (c.f. Jahn and Bovee [12, 13] and the references therein). Blake [17, 18] considered a spherical envelope model for the swimming of the protozoan opalina and the swimming motion of either a two-dimensional or cylindrical ciliated body. Miller [14, 15, 16] worked on the problem of mucus transport in the trachea by the use of a mechanical simulation of the cilia in the trachea, while an analytical model for mucus transport in the trachea had been presented by Barton and Raynor [22] without consideration of the metachronal wave motion. These studies in protozoology and mucus transport in the respiratory tract supplied information on the means of locomotion in protozoa and particle transport in the respiratory tract. However, only a little work has been done to relate the properties of the cilia and the metachronal wave to the net fluid transport in tubules. Our motivation is coming from problems associated with the understanding of the transport of fluid through the ductus efferentes of the human male reproductive tract (Greep [37]) and the effect of cilia on ovum and sperm transport in the Fallopian tubes (Blandau [20]), (Sturgis [21]). Particularly, this paper will deal with a comparison of the results for the flow rates of our model to the flow rates estimated in the ductus efferentes of the male reproductive tract.

It is to be noted that there are only a few data available on the flow rates due to ciliary activity. Based on the experimental determinations (Tuck et al. [30], Waites and Setchell [31], Setchell [33]), Lardner and Shack [4] estimated flow rate as $6 \times 10^{-3} ml/hr$ with approximate values of $R = 50\mu$, frequency of beat of the cilia as 20/sec for human testes, while the theoretical model of Lardner and Shack [4] obtained a flow rate of $0.12 \times 10^{-3} ml/hr$. Hence further studies are required for considerable improvements.

Past experimental observations indicate that most of the biological fluids possess non-Newtonian behaviour [23, 42, 43, 44, 27, 28, 29, 35]. So, analysis on the basis of simple Newtonian fluid non accurate results. The power law model is one of the simplest but the most widely used model for rheological fluid transports [24, 25, 26, 27, 28, 29, 35]. The rheological nature of this model is strongly dependent on rheological fluid index n and the model approximates both shear-thinning ($n < 1$) and shear-thickening ($n > 1$) fluids behaviour over a large range of flow conditions [42, 23, 27, 28]. Viscous properties of human semen is experimentaly found to exhibit power law-behaviour [Dunn and Picologlu [42], Mendeluk et al. [43]]. It has been reported experimently that semen proves to fit in a power-law model with pseudoplastic behavior [43, 42]. Thus studies on fluid transport of the power law model by ciliary activity may be useful to draw some important conclusions.

Recently, Siddiqui et al. [39] have studied the flow of a power law fluid due to ciliary

motion in an infinite channel and remarked that the power-law fluid gives results closer to the estimated one as $6 \times 10^{-3} ml/hr$. However, we believe that there are some drawbacks in their claim. They took $\epsilon = 0.9$, giving reference to Agarwal and Anawaruddin [40] who reported an application of their model to fluid transport in vas deferens considering $\epsilon = 0.9$. It is important to mention that ductus efferentes and vas deferens are quite different ducts, while we have no idea about the possibility of $\epsilon = 0.9$ for the later case. However, ϵ , a non-dimensional measure with respect to mean radius R of the tube and the cilia length, would be much less than $\epsilon = 0.9$ [19, 4]. To the authors' knowledge, the other drawbacks of the results in [39] are: (i) they considered large favourable pressure gradient which was constant. It is well known that pressure gradient in small biological vessels (at least when there is a wave like peristaltic wave [9, 8, 32, 28, 36], metachronal wave etc in the vessels) varies with the length of the vessels and large favourable pressure gradient are physiologically insignificant, in general, and, at least, in the ductus efferentes ([45]) (ii) Dependence of flow characteristics on δ , wave number of the metachronal wave, is not true for higher values of δ as they have done their analysis for small values of δ etc. However, their power law model is somehow different and complex to the widely used power-law model.

In view of all the above, a theoretical model for the flow in an axisymmetric tube due to metachronal wave of cilia motion has been taken into consideration for more realistic consequences. A study concerning the analysis of a non-linear problem of Ostwald-de Waele power-law fluid transport has been undertaken here by means of a sequence of cilia beat from row-to-row of cilia in a given row of cells and from one row of cells to the next (metachronal wave movement) under the conditions that the Reynolds number is small and the wave number is large.

Based upon the analytical investigation, the velocity, pressure difference, flow rate have been formulated and extensive numerical calculations have been made thereafter. Keeping in view a specific situation of fluid movement in micro-vessels by ciliary motion, the computational results are presented in graphical forms. The results presented for shear thinning and shear thickening fluids are quite relevant in the context of various studies of fluid transport due to ciliary activity. For example, semen usually behaves like shear thinning fluid when it contains a number of spermatozoa up to certain limit, however in the case of heavily concentrated spermatozoa suspensions, the fluid behaviour may be considered similar to that of a shear thickening fluid [42, 43, 44]. Moulik et al. [46] reported that high viscosity of semen can be an indication of antibodies in the plasma and/or genital tract infection.

Some novel features may be reported in this study by which we can have a better insight

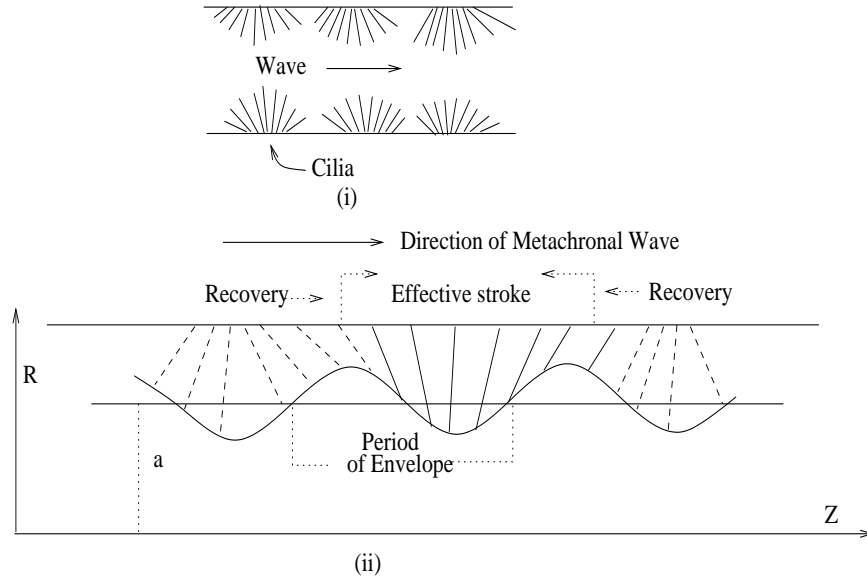


Figure 1: Wave motion of Cilia: (i) Ciliated tubule, (ii) metachronal wave pattern

of fluid motion by ciliary activity. Ciliary pumping mechanism may be utilized in the study the hydrodynamics of protozoa which use cilia for locomotion. The results may find useful applications for the possible use of cilia-based actuators as micro-mixers, for flow control in tiny bio-sensors, or as micro-pumps for drug-delivery systems.

In this investigation, the term cilia, as it is used, is limited to ciliated epithelium and will not include flagella; comparative physiology of flagella including sperm tails may be found in the papers by Fawcett [6] and by Sleight [9].

2 Formulation

A non-linear problem concerning the fluid transport characteristics in an axisymmetric tube under the action of ciliary beat that generate a metachronal wave will be studied here, by considering the fluid as an incompressible viscous non-Newtonian fluid. Let us consider an axisymmetric tube with ciliated walls of large length compared with its radius and a symplectic metachronal wave moves to the right with wave velocity c . The non-Newtonian viscous fluid behaviour within the tube is treated as an incompressible viscous Ostwald-de Waele power law type of rheological fluids.

We treat (R,θ,Z) as the cylindrical coordinates of the location of any fluid particle, R being the radius of the tube, the coordinate Z measured in the direction of wave propagation

and θ being the rotational coordinate. If τ be the stress tensor and Δ the symmetric rate of deformation tensor, the constitutive equation of shear stress for the Ostwald-de Waele power law fluid can be written as

$$\tau = \alpha \left\{ \left| \sqrt{\frac{1}{2}(\Delta : \Delta)} \right|^{n-1} \right\} \Delta, \quad (1)$$

$$\text{where } \frac{1}{2}(\Delta : \Delta) = 2 \left(\left(\frac{\partial V}{\partial R} \right)^2 + \left(\frac{V}{R} \right)^2 + \left(\frac{\partial U}{\partial Z} \right)^2 \right) + \left(\frac{\partial U}{\partial R} + \frac{\partial V}{\partial R} \right)^2$$

in which α and n denote respectively the consistency factor and the power-law index parameter, depicting the behaviour of the fluid; U and V are the velocity components in the Z and R directions. It is well known that a shear thinning fluid is classified by $n < 1$, while for a shear thickening fluid, $n > 1$. Based on the above consideration, the motion of an incompressible viscous Ostwald-de Waele power-law fluid in an axisymmetric tube together with equation of continuity may be considered to be governed by the equations

$$\frac{1}{R} \frac{\partial(R \frac{\partial V}{\partial R})}{\partial R} + \frac{\partial U}{\partial Z} = 0 \quad (2)$$

$$\rho \left(\frac{\partial U}{\partial t} + U \frac{\partial U}{\partial Z} + V \frac{\partial U}{\partial R} \right) = -\frac{\partial P}{\partial Z} + \frac{1}{R} \frac{\partial(R \tau_{RZ})}{\partial R} + \frac{\partial \tau_{ZZ}}{\partial Z} \quad (3)$$

$$\rho \left(\frac{\partial V}{\partial t} + U \frac{\partial V}{\partial Z} + V \frac{\partial V}{\partial R} \right) = -\frac{\partial P}{\partial R} + \frac{1}{R} \frac{\partial(R \tau_{RR})}{\partial R} + \frac{\partial \tau_{RZ}}{\partial Z}, \quad (4)$$

where ρ and P are the density and pressure of the fluid. Keeping the view on the geometry of the metachronal wave pattern, it is assumed that the envelope of the cilia tips can be written mathematically in the following form:

$$R = H = f(Z, t) = a + a\epsilon \cos \left(\frac{2\pi}{\lambda}(Z - ct) \right), \quad (5)$$

which can be therefore assumed as the the equation of the extensible channel wall, where ‘ a ’ denotes the mean radius of the tube, ϵ is a non-dimensional measure with respect to ‘ a ’ of the cilia length, and λ and c stand for the wave length and wave velocity of the metachronal wave. Based upon the different patterns of cilia motion observed in Sleigh (1968), the cilia tips can be considered to move in elliptical paths such that the horizontal position of a cilia tip can be written as

$$Z = g(Z, Z_0, t) = Z_0 + a\epsilon\alpha \sin \left(\frac{2\pi}{\lambda}(Z - ct) \right), \quad (6)$$

where Z_0 represents a reference position of the particle and α stands for a measure of the eccentricity of the elliptical motion. Under the no slip conditions, the velocities imparted to fluid particles are just those of the cilia tips and hence the axial and vertical velocities of the cilia can be given by

$$U = \frac{\partial Z}{\partial t}|_{z_0} = \frac{\partial g}{\partial t} + \frac{\partial g}{\partial Z} \frac{\partial Z}{\partial t} = \frac{\partial g}{\partial t} + \frac{\partial g}{\partial Z} U \quad (7)$$

$$V = \frac{\partial R}{\partial t}|_{z_0} = \frac{\partial f}{\partial t} + \frac{\partial f}{\partial R} \frac{\partial Z}{\partial t} = \frac{\partial f}{\partial t} + \frac{\partial f}{\partial Z} U \quad (8)$$

If equations (5) and (6) are applied to equations (7) and (8), we have

$$U = \frac{\frac{-2\pi a c \alpha \epsilon}{\lambda} \cos\left(\frac{2\pi}{\lambda}(Z - ct)\right)}{1 - \frac{2\pi a \alpha \epsilon}{\lambda} \cos\left(\frac{2\pi}{\lambda}(Z - ct)\right)} \quad (9)$$

$$V = \frac{2\pi c \sin\left(\frac{2\pi}{\lambda}(Z - ct)\right)}{1 - \frac{2\pi a \alpha \epsilon}{\lambda} \cos\left(\frac{2\pi}{\lambda}(Z - ct)\right)} \quad (10)$$

These boundary conditions enable us to distinguish between the effective stroke of the cilia and the slow less effective recovery stroke by approximately accounting for the shortening of the cilia. In other words, we can say that the tube is narrower when U is positive.

For a wave frame (z, r) moving with a velocity c away from a fixed frame (Z, R) , let us take the transformations

$$z = Z - ct, \quad r = R, \quad u = U - c, \quad v = V, \quad p(z, t) = P(Z, R, t) \quad (11)$$

in which (u, v) and (U, V) are the velocity components, p and P stand for pressure in wave frame and fixed frame of reference respectively. Henceforward, we shall make use of the following non-dimensional variables:

$$\begin{aligned} \bar{z} = \frac{z}{\lambda}, \quad \bar{r} = \frac{r}{a}, \quad \bar{u} = \frac{u}{c}, \quad \bar{v} = \frac{v}{c\delta}, \quad \delta = \frac{a}{\lambda}, \quad \bar{p} = \frac{a^{n+1}p}{\alpha c^n \lambda}, \quad \bar{t} = \frac{ct}{\lambda}, \quad h = \frac{H}{a}, \\ Re = \frac{\rho a^n}{\alpha c^{n-2}} \frac{a}{\lambda}, \quad \bar{\tau}_{rz} = \frac{\tau_{rz}}{\alpha \left(\frac{c}{a}\right)^n}, \quad \bar{Q}_1 = \frac{Q_1}{\pi a^2 c} \end{aligned} \quad (12)$$

If we drop the bars over these symbols, the equations governing the flow of the fluid can be rewritten as

$$\frac{1}{r} \frac{\partial(r \frac{\partial v}{\partial r})}{\partial r} + \frac{\partial u}{\partial z} = 0 \quad (13)$$

$$Re \left(\frac{\partial u}{\partial t} + u \frac{\partial u}{\partial z} + v \frac{\partial u}{\partial r} \right) = -\frac{\partial p}{\partial z} + \frac{1}{r} \frac{\partial \left(\Phi \left(r \frac{\partial u}{\partial r} + r \delta^2 \frac{\partial v}{\partial z} \right) \right)}{\partial r} + 2\delta^2 \frac{\partial \left(\Phi \frac{\partial u}{\partial z} \right)}{\partial z} \quad (14)$$

$$Re\delta^2 \left(\frac{\partial v}{\partial t} + v \frac{\partial v}{\partial z} + v \frac{\partial v}{\partial r} \right) = -\frac{\partial p}{\partial r} + \delta^2 \frac{1}{r} \frac{\partial(r\Phi \frac{\partial v}{\partial r})}{\partial r} + \delta^2 \frac{\partial \left(\Phi \left(\frac{\partial u}{\partial r} + \delta^2 \frac{\partial v}{\partial z} \right) \right)}{\partial z} \quad (15)$$

$$\Phi = \left| \sqrt{2\delta^2 \left\{ \left(\frac{\partial v}{\partial r} \right)^2 + \left(\frac{v}{r} \right)^2 + \left(\frac{\partial u}{\partial z} \right)^2 \right\} + \left(\frac{\partial u}{\partial r} + \delta^2 \frac{\partial v}{\partial z} \right)^2} \right|^{n-1} ; \quad (16)$$

whereas the boundary conditions are

$$\frac{\partial u}{\partial r} = 0 \text{ at } r = 0 \text{ and } u = \frac{-2\pi\alpha\delta\epsilon \cos(2\pi z)}{1 - 2\pi\alpha\delta\epsilon \cos(2\pi z)} - 1 \quad (17)$$

$$v = \frac{2\pi \sin(2\pi z)}{1 - 2\pi\alpha\delta\epsilon \cos(2\pi z)} \quad (18)$$

on $r = h = 1 + \epsilon \cos(2\pi z)$.

Since in most of the cases of flow in small diameter tubules, Reynolds numbers are very small ($Re \ll 1$), the analysis can be carried out by the approximation of the inertia-free flow. In this case, the governing equations under the consideration of the long-wavelength approximation can be simplified as follows:

$$0 = -\frac{\partial p}{\partial z} + \frac{1}{r} \frac{\partial(r \frac{\partial u}{\partial r} |\frac{\partial u}{\partial r}|^{n-1})}{\partial r} \quad (19)$$

$$0 = -\frac{\partial p}{\partial r} \quad (20)$$

and also the forms of the boundary conditions will now be

$$\frac{\partial u}{\partial r} = 0 \text{ at } r = 0 \text{ and } u = u(h) = -1 - 2\pi\alpha\delta\epsilon \cos(2\pi z) \quad (21)$$

$$v = v(h) = 2\pi\epsilon \sin(2\pi z) + 4\pi^2\epsilon^2\alpha\delta \sin(2\pi z) \cos(2\pi z) \quad (22)$$

on $r = h = 1 + \epsilon \cos(2\pi z)$. By solving (19) subject to the boundary condition (9), we have found the axial velocity in the form

$$u(r, z) = u(h) + \frac{p|p|^{k-1}}{2^k(k+1)} [r^{k+1} - h^{k+1}] \quad (23)$$

If we integrate the continuity (19) across the cross section of the tube, we get

$$2 \int_0^h \frac{1}{r} \frac{\partial(r \frac{\partial v}{\partial r})}{\partial r} r dr + 2 \int_0^h \frac{\partial u}{\partial z} r dr = 0 \quad (24)$$

$$\text{or, } rv|_h - rv|_0 + \frac{\partial}{\partial z} \int_0^h u r dr - hu(h, z, t) \frac{\partial h}{\partial z} - 0 \times u(0, z, t) \times \frac{\partial 0}{\partial z} = 0 \quad (25)$$

$$\text{or, } hv(h) + \frac{1}{2} \frac{\partial q}{\partial z} - h \frac{\partial h}{\partial z} u(h) = 0, \text{ where } q = 2 \int_0^h u r dr \quad (26)$$

$$\text{which implies that } \frac{\partial q}{\partial z} = 2h \left(\frac{\partial h}{\partial z} u(h) - v(h) \right) = 0. \quad (27)$$

This shows that the volume flow rate q in the wave frame of reference is constant. On integration (23) across the cross section of the tube, the pressure gradient can be represented in terms of the volume flow rate by the following form.

$$q = h^2 u(h) - \frac{p|p|^{k-1} h^{k+3}}{2^k(k+3)} \quad (28)$$

Putting dp/dz , obtained from (28), into (23) we calculate

$$u(r, z) = u(h) + \frac{(k+3)(q - h^2 u(h))}{(k+1)h^{k+3}} [h^{k+1} - r^{k+1}] \quad (29)$$

The instantaneous volume flow rate, $Q_1(Z, t)$, in the fixed frame of reference is found by integrating

$$Q_1(Z, t) = 2 \int_0^h U(R, Z, t) R dR = q + h^2 \text{ (using the transformation formulas (11))} \quad (30)$$

Thus, the time-mean volume flow over a period is given by

$$Q(Z, t) = \frac{1}{T} \int_0^T Q_1(Z, t) dt = q + \frac{1}{T} \int_0^T h^2(Z, t) dt \quad (31)$$

which, on integration for the sinusoidal wall of (5), gives

$$Q(Z, t) = q + 1 + \frac{\phi^2}{2} \quad (32)$$

After solving dp/dz from (28) and using (32), the pressure rise per wavelength can be calculated by the relation

$$\Delta p = \int_0^1 \frac{dp}{dz} dz = - \int_0^1 \left| \frac{2^k(k+3)(Q - 1 - \frac{\phi^2}{2} - h^2 u(h))}{h^{k+3}} \right|^{n-1} \left\{ \frac{2^k(k+3)(Q - 1 - \frac{\phi^2}{2} - h^2 u(h))}{h^{k+3}} \right\} dz. \quad (33)$$

It may be noted that if we put $n = 1$, $\alpha = 0$ in Equations (23), (28) and (33), the expressions reduce to those reported earlier in Ref. [32]. If $\alpha = 0$, the results also match well those of Ref. [27] when the peristaltic wave form in [27] is replaced by the metachronal wave in this study in the fixed frame of reference. Similarly, if the yield stress is set equal to zero and fluid flow is considered in an axisymmetric uniform vessel in [36], the expressions said above reduces to that obtained in [36].

By solving the continuity equation (13) subject to the boundary condition (22), we have found the radial velocity as

$$v(r, z) = u(h) \frac{r^{k+2}}{h^{k+2}} \frac{\partial h}{\partial z} + \frac{h}{k+1} \left[\frac{r}{h} - \frac{r^{k+2}}{h^{k+2}} \right] \frac{\partial u(h)}{\partial z} + \frac{(k+3)q}{(k+1)h^2} \left[\frac{r}{h} - \frac{r^{k+2}}{h^{k+2}} \right] \frac{\partial h}{\partial z} \quad (34)$$

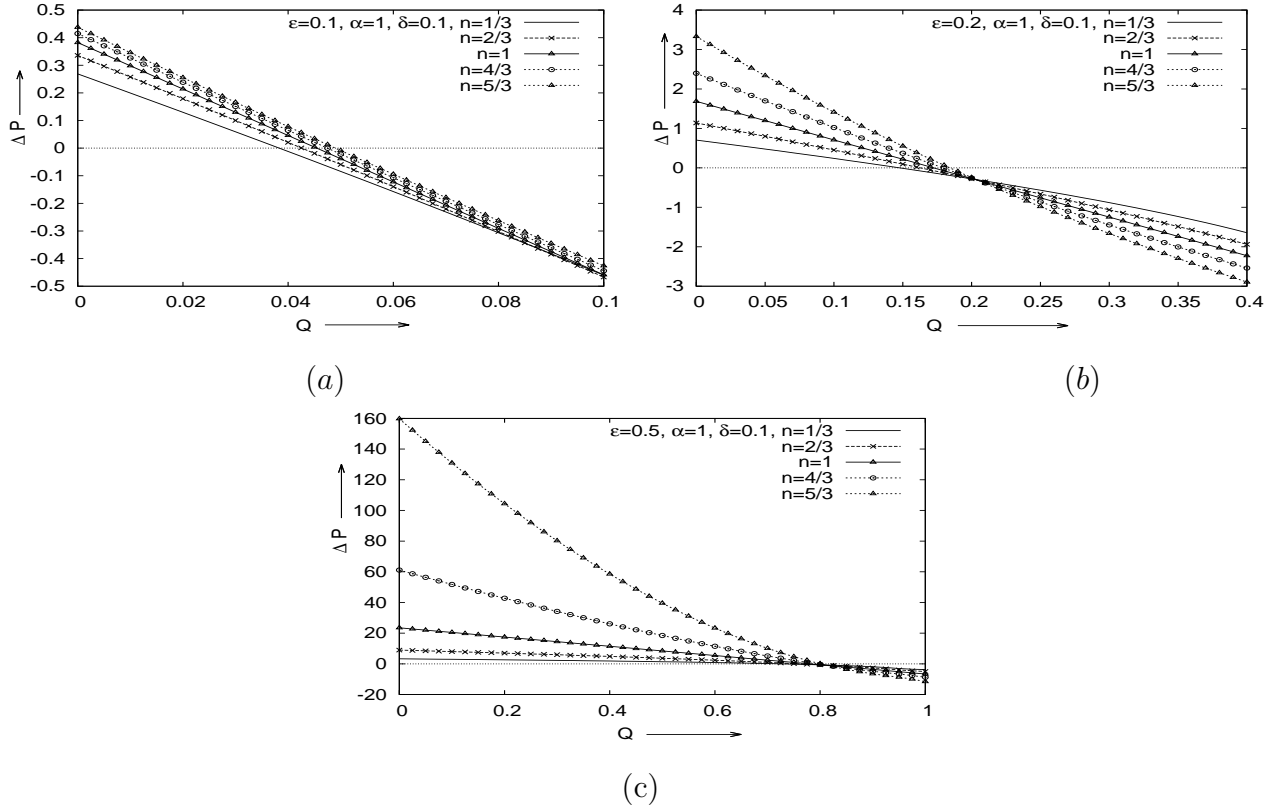


Figure 2: The diagrams exhibit the dependence of flow rate and pressure difference relation ($Q - \Delta p$) on ϵ , flow behaviour index n and eccentricity α . In all the figures, wave number $\delta = 0.1$, $\alpha = 1$ and n has been varied from $1/3$ to $5/3$ to observe the changes taking place in $Q - \Delta p$ relation. Effect of ϵ on $Q - \Delta p$ relation has been shown in Figs. (a-c) by varying ϵ from 0.1-0.5.

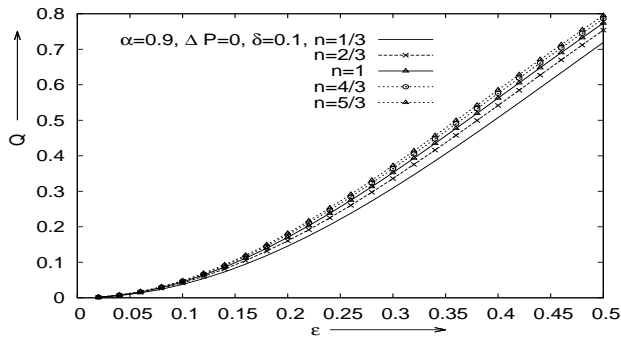


Figure 3: The diagram exhibits the dependence of flow rate Q and ϵ relation on flow behaviour index n by plotting graphs for $n=1/3-5/3$. The other parameters are kept as $\Delta p = 0$, i.e. free pumping, $\delta = 0.1$, $\alpha = 0.9$.

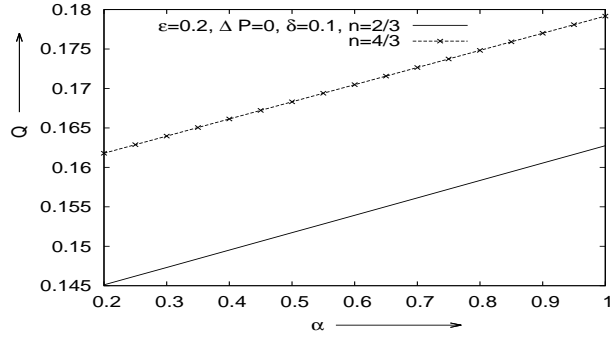


Figure 4: The diagram exhibits the dependence of flow rate Q and eccentricity α relation on flow behaviour index n by plotting graphs for $n=2/3-4/3$. The other parameters are kept as $\Delta p = 0$, i.e. free pumping, $\delta = 0.1$, $\epsilon = 0.2$.

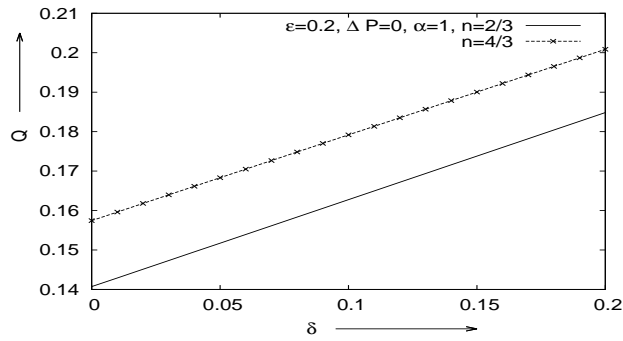


Figure 5: The diagram exhibits the relation of flow rate Q with wave number δ and its dependence on flow behaviour index n , which has been shown by plotting graphs for $n=2/3$ and $4/3$. The other parameters are kept as $\Delta p = 0$, i.e. free pumping, $\alpha = 1$, $\epsilon = 0.2$.

3 Quantitative Study

This section deals with a quantitative analysis of the mathematical model presented in the earlier sections. It may be noted that unlike the Newtonian model, in Ostwald-de Waele power law model it has been not possible to find an explicit analytical expression of pressure difference Δp in terms of time averaged flow rate \bar{Q} due to the complexity of the problem of a rheological fluid when the wave shape is arbitrary. However, a numerical computation is required to express pumping characteristics or pumping performance of the rheological fluid for a clear understanding. In addition, it is a convention to exhibit velocity field in term of the pressure difference between the tube ends. Hence, in view of those observations and to fulfill the demands, necessary computations have been carried out numerically by using the software MATHEMATICA.

It is to be noted that there is only a few available data on the flow rates due to ciliary activity [4, 19]. For the quantitative study, we shall present theoretical estimates of different physical quantities that are of relevance to physical problems of the flows of rheological fluids under ciliary activity. On the basis of the present analysis, the following non-dimensional data for the rheological fluids have been used [4, 19]:

$$\epsilon = 0.1 \text{ to } 0.5, \alpha = 0.3 \text{ to } 1, \delta = 0.05 \text{ to } 0.2, n = \frac{1}{3} \text{ to } 2, \bar{Q} = 0 \text{ to } 1.$$

3.1 Pumping Characteristics

It is natural that pressure-flow characteristic (i.e. the pumping characteristics) can be determined through the variation of time averaged flow rate \bar{Q} with difference in pressure ΔP across one wave length. The variations of volumetric flow rate of the fluid by cilia motion, for different values of ϵ , flow index number n , wave number δ and eccentricity α are exhibited in Figs. 2. As expected to the linear nature of the case inertia-free flow ($Re=0$) of a Newtonian fluid, the curve of ΔP versus \bar{Q} is a straight line with negative slope and positive intercepts; however, for the aforesaid case of a rheological (non-Newtonian) fluid the relationship between the pressure difference and the mean flow rate is nonlinear.

The curves have three portions, namely, (i) free pumping zone, describing the region in which $\Delta P = 0$, (ii) pumping zone, indicating the region where $\Delta P > 0$ and (iii) co-pumping zone, which regarded for the region where $\Delta P < 0$, the situation favourable for the flow to take place. From the above said relation, it is possible to calculate the amount of flow pumped by ciliary activity, even in the absence of mean pressure gradient ($\Delta P = 0$) and also in the presence of adverse pressure gradient (i.e $\Delta P > 0$) up to certain a limit. If ϵ , n , δ , α are fixed

at some values imposition of an adverse mean pressure gradient reduces the mean flow rate relative to the value obtained during free pumping and when it is large enough (certain limit), it balances exactly the driving force for flow produced by the cilia motion, and the mean flow rate is zero. Whereas if ΔP (> 0) exceeds this limit, the flow will take place in the backward direction.

Figs. 2(a-c) show that the area of the pumping region and the length of the free pumping zone both increase significantly with a rise in ϵ for Newtonian, shear thinning as well as shear thickening fluids and also these (area, length) enhance at a very high rate with an increase in the rheological parameter n . In other words, for fixed values of ΔP , time averaged flow rate \bar{Q} rises with an increase in ϵ and n . However, in the co-pumping zone, there is a critical value of ΔP for higher values of ϵ (> 0.1) up to which \bar{Q} for fixed values of ΔP can be raised with an increase in n and if ΔP exceeds this critical value the reverse trend occurs. It is important to mention that for fixed values of parameters taken by Lardner and Shack together with $n = 1$, the flow rate in axisymmetric tube is two times more than the values reported by Lardner and Shack for a two-dimensional channel. In the case of free pumping, Fig. 2(d) clearly reveals that there is a remarkable enhancement of flow rate with increase in ϵ . It further explains that n strongly influences the flow rate. The plots, presented in Figs. 2(e-f), indicate that for a non-Newtonian fluid, \bar{Q} increase as the wave number δ and ϵ increase and these parameters enhance \bar{Q} at almost the same rate for both the shear thinning and shear thickening fluids.

It is worthwhile to mention that an increase of ϵ corresponds to rise of cilia length and vice versa. Again in the case of free pumping, when $\epsilon=0$, there is no cilia to the inner surface of the tube, then $\bar{Q}=0$.

3.2 Distribution of Velocity

As shown in previous section, the mean flow is attributable solely to the motion of ciliary activity during free pumping and motion of cilia supplies the only driving force for fluid motion. The distributions of axial velocity for the present study are plotted in Figs. (6-10) for different values of ϵ , n , δ and α . Since the flow is unsteady in the fixed frame of reference and the velocity profiles along with the radius of the blood vessels change with time, the distribution of velocity has been investigated at a time interval of a quarter of a metacronal wave period of cilia.

One can observe from Fig. 6 that at any instant of time, there exists a retrograde flow region and the maximum retrograde flow occurs at the narrowest portion of the tube, while

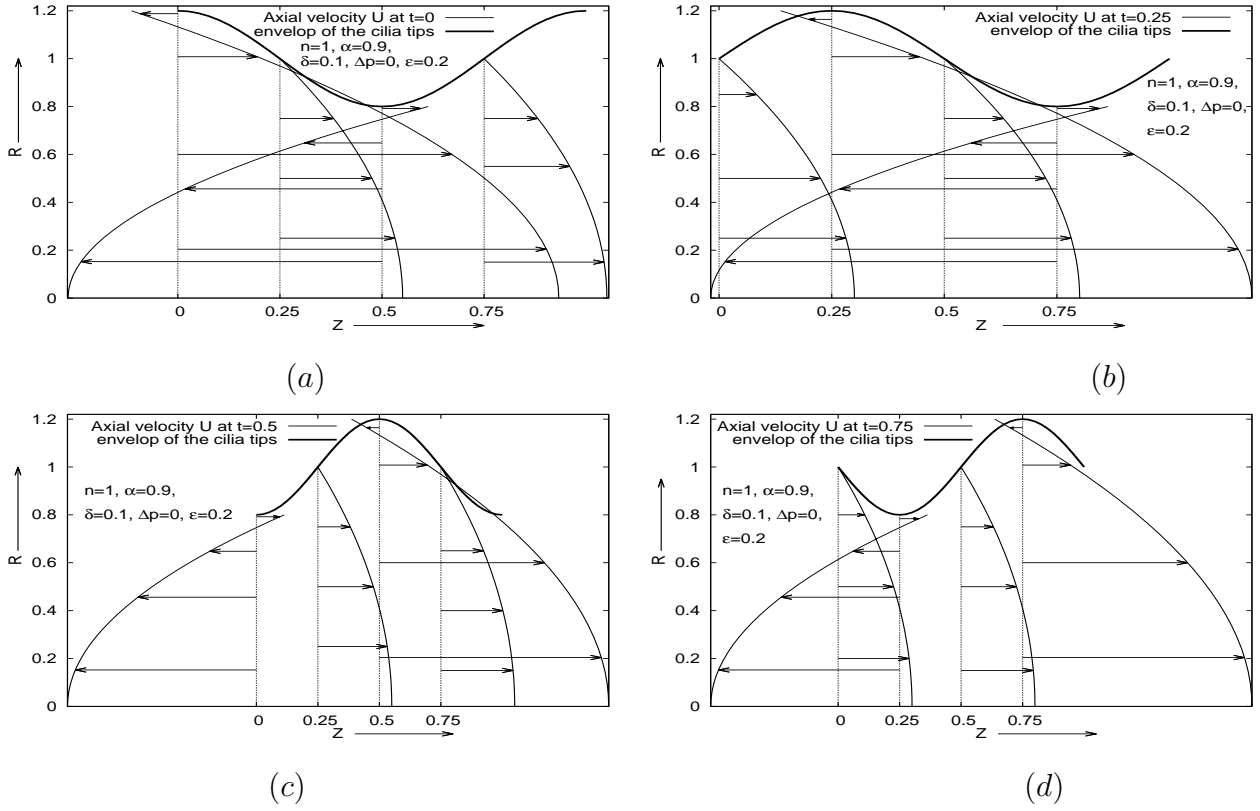


Figure 6: The diagrams exhibit velocity profiles along the tube axis corresponding to the axial positions indicated by vertical lines, (based on equation (29)) at different instants of time ($t=0.0-0.75$). The dark coloured curves represent envelop of cilia tips. Arrows indicate the direction of velocity. Reversal of flow corresponding a velocity profile has been indicated by reversed arrows in the vicinity of the envelop.

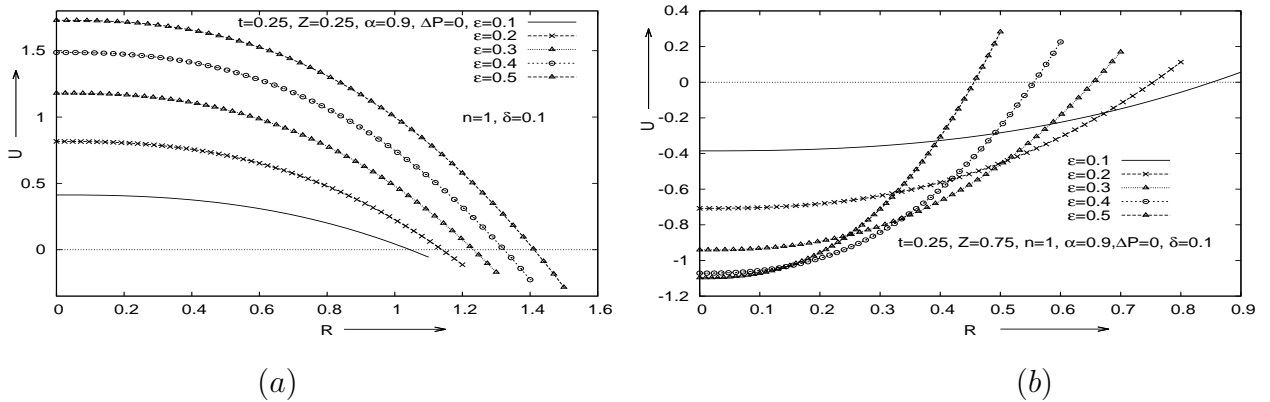


Figure 7: The diagrams show the distributions of velocities of a Newtonian fluid at the wave crest and the wave trough section for the different values of ϵ when $\Delta P = 0$.

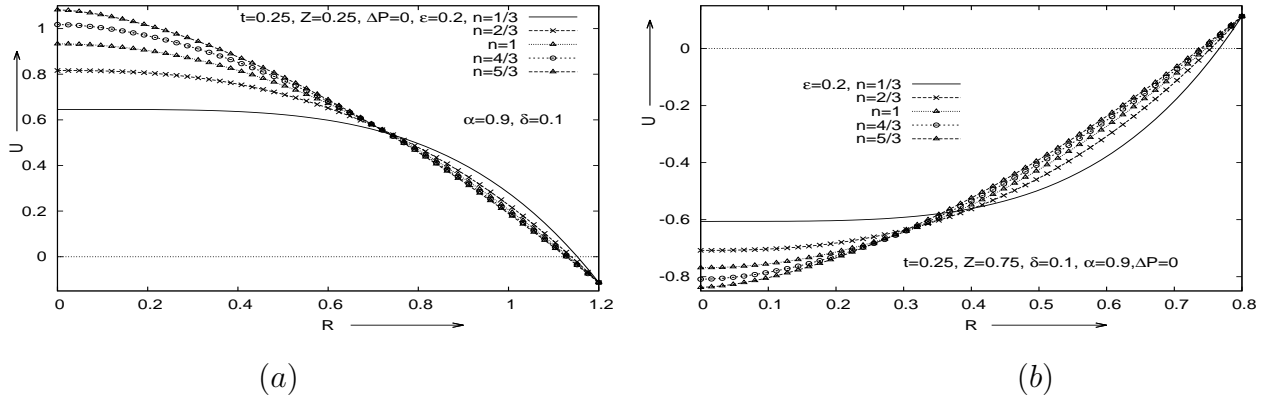
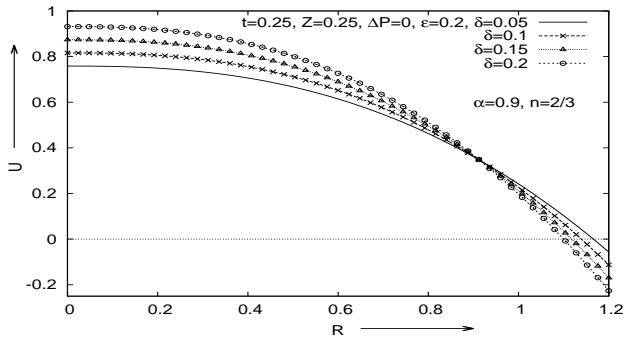


Figure 8: The diagrams exhibit the velocity profiles of the rheological fluids at the wave crest and the wave trough sections for the different values of n .

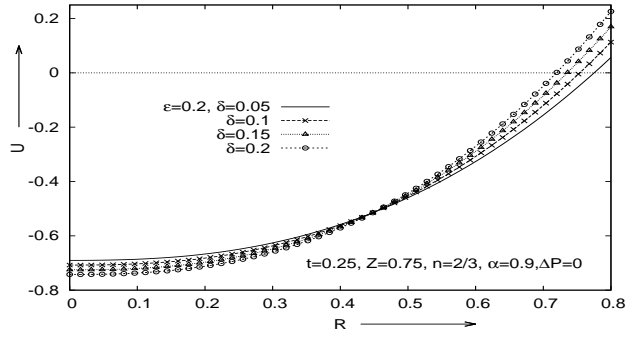
the maximum forward flow occurs at the widest portion of the tube. However, the forward flow region is predominant in this case, since the time-averaged flow rate is positive for free-pumping (cf. Pumping Characteristic in the previous section). Moreover, the study further reveals that there exist two stagnation points on the axis. For example, at time $t=0.75$, one of the stagnation points lies between $Z=0.0$ and $Z=0.25$, while the other lies between $Z=0.25$ and $Z=0.5$ separating the central region of a retrograde flow from two forward flow regions. Similar observations were made numerically and analytically by Takabatake and Ayukawa [34] and Maiti and Misra [35, 36], Misra and Maiti [28] for a Newtonian fluid and non-Newtonian fluids respectively for a peristaltic transport. From the standpoint of ciliary pumping, this retrograde flow at the trough region is considered to be a kind of ineffective leakage.

It is to be noted that the beat of a single cilium can be separated into two distinct phases. One being the effective stroke of cilia, when the cilium moves in the same direction as the general fluid movement and the reflux may occurs near the walls and in this case the portion of tube is wider. The other phase being the recovery stroke, when the cilium moves in opposite direction to general fluid movement and there may be forward flow near the walls and in this case the portion of the tube is narrower.

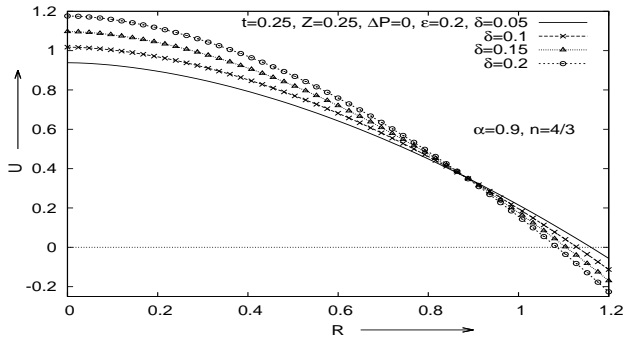
The effects of ϵ , n , δ and α upon the velocities at the crest and the trough section of the tube are shown in Figs. (7-10) in the case of free-pumping. It may be observed from the Fig. (7) that there is a remarkable increase in magnitude of the axial velocity due to an increase in the value of ϵ for both sections. This implies that the increase of cilium length at least up to a certain limit can produce more driving force. Fig. (8) illustrates that the magnitude of the



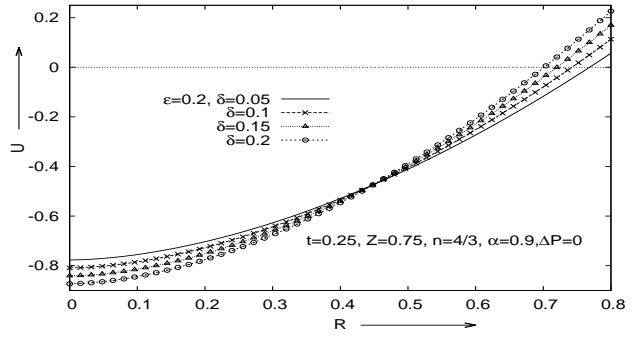
(a)



(b)



(c)



(d)

Figure 9: The diagrams exhibit the velocity profiles of the rheological fluids at the wave crest and the wave trough sections for the different values of δ .

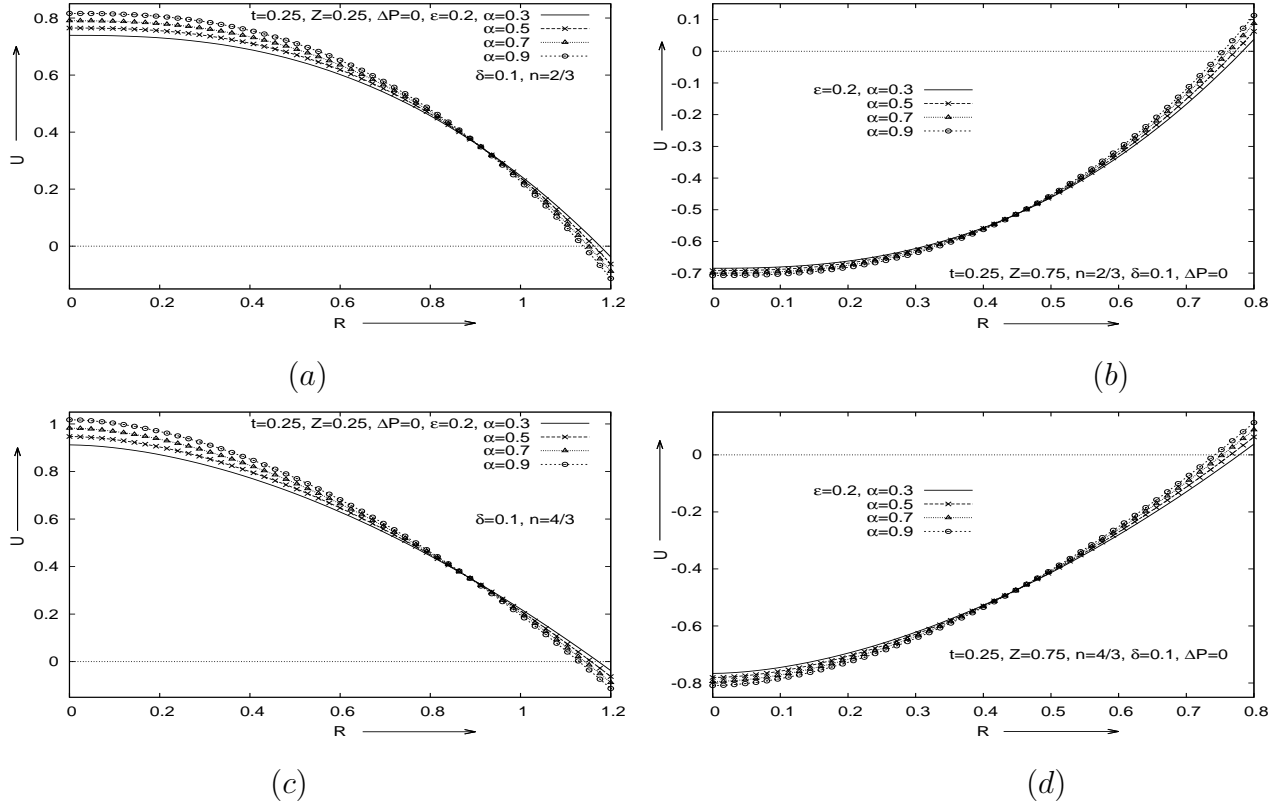


Figure 10: The diagrams exhibit the velocity profiles of the rheological fluids at the crest and the trough section for the different α values of α .

axial velocity for both sections enhances significantly at the central region, while the reverse trend occurs at the boundary region if flow index number n increases. That reverse trend might have been initiated due to the increase of friction at the boundary region of the tube if n rises. As shown in Figs. (9-10), for both sections, wave number δ and eccentricity α of the path of the cilia raise the magnitude of the axial velocity at the central region, while at the boundary region the trend is reversed indicating the rise of friction by increase in δ and α .

4 Application to fluid transport in the ductus efferentes

The ciliated walls of an axisymmetric tube have been modelled by a metachronal wave of cilium which is equivalent to a wavy wall of peristaltic transport. There is only a few available data in the existing literature on the flow rates due to the ciliary activity. The relationship between the pressure difference and the time-mean-volume flow through an axisymmetric tube

is given in (33). We have to test if the results of (33) are applicable to the flow rates observed in the ductus efferentes of the male reproductive tract. In the human, the ductuli efferentes are 10-15 tubules connecting the rete testis to the epididymis and the cells lining these tubules are ciliated. It is generally believed that the cilia are responsible for fluid transport [37]. On the basis of experimental observations [30, 31, 33] on the flow rates in the rete testis of rat, ram, and bull, the approximate flow rate in human rete testis per ductus efferentes was estimated by Lardner and Shack [4] as $6 \times 10^{-3} \text{ ml/h}$ with approximate dimensions of $R = 50 \mu\text{m}$, with frequency of beat of the cilia being 20/sec and $c = (20 \text{ beats/sec}) \times 10 \mu = 200 \mu/\text{sec}$. The said values justify the use of long wavelength and small Reynolds number theory ($Re \ll 1$) of the study. Lardner and Shack [4] calculated the non-dimensional flow rate and dimensional flow rate as 2.2×10^{-2} and $0.12 \times 10^{-3} \text{ ml/h}$ respectively from their model in the case of free pumping assuming $\epsilon = 0.1$, $\delta = 0.1$ and $\alpha = 1$. However, if we consider all these values fixed with our model together with $n = 1$, our model gives the non-dimensional flow rate in an axisymmetric tube as 4.54514×10^{-2} and consequently the dimensional flow rate is $0.257 \times 10^{-3} \text{ ml/h}$ (cf. Fig. 2a). These values, for an axisymmetric tube are twice the values reported by Lardner and Shack [4] for a two-dimensional channel. Thus a considerable improvement is needed. However, ϵ is linearly proportional to the cilia length on the basis of the assumption and n is linked to the rheological fluid (widely known as non-Newtonian fluid) in the ductus efferentes of the male reproductive tract. It has been seen from Fig. 2 that the flow rates increase significantly with an increase in ϵ . The flow rates increase with cilia length was also reported in [19]. Moreover, for higher values of ϵ , rheological fluid index n remarkably affect the fluid transport for adverse pressure gradient at pumping zone. In addition, if we consider $n = 4/3$, $\epsilon = 0.5$, $\Delta P = 0$, $\delta = 0.1$ and $\alpha = 1$ then the non-dimensional flow rate and dimensional flow rate are calculated as 0.792614 and $4.482 \times 10^{-3} \text{ ml/h}$ respectively which is close to the estimated value $6 \times 10^{-3} \text{ ml/h}$. But authors have no idea about the actual length of cilia and hence the value of ϵ , due to non-availability of real physiological data of the concerned variables and parameters used in the analysis.

5 Summary and Conclusion

An analysis for the rheological fluid transport by means of a sequence of beat of cilia which are in an array and coordinated in such a way as to represent the metachronal wave is presented. The objective of the present study is related to the problems associated with the understanding of

the fluid transport through the ductus efferentes of the human male reproductive tract ([37, 41]) and the effect of cilia on ovum and sperm transport in the Fallopian tubes etc. However aonly n application of the our results for flow rates to the observed flow rates in the ductus efferentes of the reproductive tract is discussed here. On the basis of the derived analytical expressions, extensive numerical computations have been carried out. The effects of various parameters, such as ϵ , n , δ , α on pumping characteristic and velocity distribution are investigated in detail in the case of an axisymmetric tube flow.

The study reveals that for a particular set of values, say $\epsilon = 0.1$, $\delta = 1$, $\alpha = 1$, $n = 1$, $\Delta P = 0$, as considered in [4], flow rate in an axisymmetric tube is twice the value reported by Lardner and Shack [4] for a two-dimensional channel. It further reveals that the flow rate changes remarkably with ϵ and n and when ϵ is near by 0.5 our results of flow rate in human ductus efferentes are close to the estimated value $6 \times 10^{-3} \text{ ml/h}$ as suggested by Lardner and Shack [4] based on the experimental observations on the flow rates in the ductus efferentes in the other animals e.g. rat, ram, and bull.

The considerable difference between the theoretical and the observed values indicates that the metachronal wave of cilia cannot account for the total flow rate in ductus efferents and there must be some other important factors, responsible for the transport of semen. These factors may be (cf. Ilio and Hess [41]) (a) contraction of smooth muscle (b) constant secretion of fluid by the seminiferous epithelium (c) contraction of the myoepithelial layer of the seminiferous tubule and tunica albuginea of the testis (d) the vacuum created by the ejaculation of sperm from the lower tract and by the absorption of fluid (e) increased pressure due to the pattern of branching and convergence of ductuli. Consequently, to understand the mechanism involved in transport of semen in ductus efferentes of male repductive tract adequately, further theoretical and experimental investigations are essential. It is important to mention that forward flow takes place at the wider portion of the tube, while backward flow occurs at narrower portion of the tube in a similar fashion of peristaltic transport [34, 27, 28, 36], although forward flow is dominant for positive time-averaged flow.

Acknowledgment: *One of the authors, S. Maiti, is grateful to the University Grants Commission (UGC), New Delhi for awarding the Dr. D. S. Kothari Post Doctoral Fellowship during this investigation.*

References

- [1] Rivera, J. A, *Cilia, Ciliated Epithelium, and Ciliary Activity*. New York: Pergamon Press (1962)
- [2] Gray, J, *Ciliary Movement*, New York: Academic Press (1928).
- [3] Lucas, A . M, Ciliated Epithelium, *Special Cytology* **1** (1932), 409-473.
- [4] Lardner T. J. and Shack W. J., Cilia transport, *Bull. Math. Biol* **34** (1972), 325-335.
- [5] Faure-Fremiet, E, Cils Vibratiles et Flagelles, *Biol. Rev.* **36** (1961), 464-436.
- [6] Fawcett, D., *Cilia and Flagella*, In *The Cell*, Braehet, J. and A. E. Mirsky, eds. New York: Academic Press (1961).
- [7] Satir, P., Structure and Function in Cilia and Flagella, *Protoplasmatologia*, IIIE (1965).
- [8] Satir, P., Studies of Cilia; The Fixation of the Metachronal Wave, *J. Cell Biology* **18** (1963), 345-365.
- [9] Sleight, M. A, *The Biology of Cilia and Flagella*, New York: MacMillan (1962).
- [10] Sleight, M. A, Patterns of Ciliary Beating, In *Aspects of Cell Motility*, pp. 131. Soc. Expl. Biol. Symp. X X I I . New York: Academic Press (1968).
- [11] Borell, U., O. Milsson, and Westman. A, Ciliary Activity in the Rabbit Fallopian Tube During Oestrus and After Copulation, *Acta Obst. Gynee. Scand.* **36** (1957), 22-28.
- [12] Jahn, T. L. and Bovee, E. C., Movement and Locomotion of Microorganism, *Ann. Rev. Microbiology* **19** (1965), 21-58.
- [13] Jahn, T. L. and Bovee, E. C., *Motile Behaviour of Protozoa*, In *reeseearch in proto-zoology*, Vol. 1. New York: Pergamon Press, pp. 40 (1967).
- [14] Miller, C. E, An Investigation of the Movement of Newtonian Liquids Initiated and Sustained by the Oscillation of Mechanical Cilia, *Prec. 5th Cong. Appl. Mech.* (1966), 715-720.
- [15] Miller, C. E, An Investigation of the Movement of Newtonian Liquids Initiated and Sustained by the Oscillation of Mechanical Cilia, *Aspen Emphysema Conf.* (1967), 309-321.

- [16] Miller, C. E, Streamlines, Steak Lines and Particle Pathlines Associate with a Mechanically-induced Flow Holomorphic with the Mammalian Mucociliary System, *Biorheology* **6** (1969), 127-135.
- [17] Blake, J. R., A model for the microstructure in ciliated micro-organisms, *J. Fluid Mech.* **55** (1972), 1-23.
- [18] Blake, J. R., A Spherical Envelope Approach to Ciliary Propulsion, *J. Fluid Mech.* **46** (1971), 199-208.
- [19] Blake, J. R., Flow in tubules due to ciliary activity, *Bull. Math. Biol* **35** (1973), 513-523.
- [20] Blandau, 1969. R. J., *Gamete Transport—Comparative Aspects*, In The Mammalia Oviduct, Hafez, E. S. and Blandau, R. J. eds. Chicago: Univ. of Chicago Press, 129-162 (1969).
- [21] Sturgis, S. H., The Effect of Ciliary Current on Sperm Progress in Excised Human Fallopian Tubes, *Trans. Amer. Soc. Study Sterility*, **3** (1947), 31-39.
- [22] Barton, C. and Raynor, S, Analytical Investigation of Cilia Induced Mucous Flow, *Bull. Math. Biophysics* **29** (1967), 419-428.
- [23] Malek J., Necas J. and Rajagopal K. R., Global existence of solutions for fluids with pressure and shear dependent viscosities, *Appl. Math. Let.* **15** (2002), 961-967.
- [24] Srivastava, L. M and Srivastava V. P., Peristaltic transport of a power-law fluid: Application to the ductus efferentes of the reproductive tract, *Rheol. Acta* **27**(4) (1988), 428-433.
- [25] Usha, S. and Rao A. R., J Biomech Eng. 1997 Nov;119(4):483-8. Peristaltic transport of two-layered power-law fluids, *J. Biomech. Eng.* **119**(4) (1988), 483-488.
- [26] Rao, A. R. and Mishra, M., Peristaltic transport of a power-law fluid in a porous tube, *J. Non-Newtonian. Fluid Mech.* **33**(3) (2012), 15-32.
- [27] Misra J. C. and Maiti S., Peristaltic transport of rheological fluid: model for movement of food bolus through esophagus, *Appl. Math. Mech.* **121**(2-3) (2004), 163-174.
- [28] Misra J. C. and Maiti S., Peristaltic pumping of blood through small vessels of varying cross-section, *Trans. ASME J. App. Mech.* **22**(8) (2012), 061003 (19 pages).

- [29] Misra J. C. and Pandey S. K., Peristaltic flow of a multi-layered power-law fluid through a cylindrical tube, *Int. J. Engn. Sci.* **39** (2001), 387-402.
- [30] Tuck R. R, Setchel B. P, Waites G. M. H, Young J. A, The Composition of Fluid Collected by Micropuncture and Catherization from the Seminiferous Tubules and Rete Testis of Rats, *Pflugers Arch.*, **318** (1970), 225-243.
- [31] Waites, G. M. H. and Setchell, P. P., *Some Physiological Aspects of the Function of the Testis*, In *The Gonads*, K. W. McKerns, ed. New York: Appleton (1969)
- [32] Shapiro A. H. Jaffrin M. Y. and Weinberg S. L., Peristaltic pumping with long wavelength at low Reynolds number, *J. Fluid Mech.* **37** (1969), 799-825.
- [33] Setchell, B. P., *Testicular Blood Supply, Lymphatic Drainage, and Secretion of Fluid*, *The Testis*, Vol. 1. (1970).
- [34] Takabatake S. and Ayukawa K., Numerical study of two-dimensional peristaltic flows, *J. Fluid Mech.* **122** (1982),
- [35] Maiti S., Misra J. C., Peristaltic Transport of a Couple Stress Fluid: Some Applications to Hemodynamics, *J. Mech. Med. Biol.* **12**(3) (2012), 1250048 (21 pages).
- [36] Maiti S., Misra J. C., Non-Newtonian characteristics of peristaltic flow of blood in microvessels, *Commun. Nonlinear Sci. Numer. Simul.* **18** (2011), 1970-1988.
- [37] Greep, R. D., *Histology*. New York: Blakiston Division, McGraw-Kill. (1983)
- [38] Provost A. M. and Schwarz W. H., A theoretical study of viscous effects in peristaltic pumping, *J. Fluid Mech.* **279** (1994), 177-195.
- [39] Siddiqui, A. M, Haroon, T, Rani, R and Ansari A. R, An analysis of the flow of a power law fluid due to ciliary motion in an infinite channel, *Commun. Non-linear Sci. Numer. Simul.* **16** (2011), 3107-3125.
- [40] Agarwal H. and Anawaruddin, Cilia transport of bio-fluid with variable viscosity, *Indian J Pure Appl Math.* **15**(10) (1984), 1128-1139.
- [41] Ilio, K. Y. and Hess R. A, Structure and Function of the Ductuli Efferentes: A Review, *Microscopy Res. Tech.* **29** (1994), 432-467.

- [42] Dunn, P. F. and Picologlou, B. F, Investigation of rheological properties of human semen, *Biorheology* **14** (1977), 277-292.
- [43] Mendeluk G, Flecha, F. L. G, Castello, P. R. and Bregni, C., Factors Involved in the Biochemical Etiology of Human Seminal Plasma Hyperviscosity, *Journal of Andrology* **21**(2) (2000), 262-267.
- [44] Xue, H., The modified Casson's equation and its application to pipe flows of shear thickening fluid, *Acta Mechanica Sinica* **21** (2005), 243-248.
- [45] Winet, H., On the mechanism for flow in the efferent ducts, *J. Andrology* **1**(6) (1980), 304-311.
- [46] Moulik S, Gopalkrishnan K, Hinduja I, Shahani SK, Presence of sperm antibodies and association with viscosity of semen, *Hum Reprod.* **4** (1989), 290-291.